























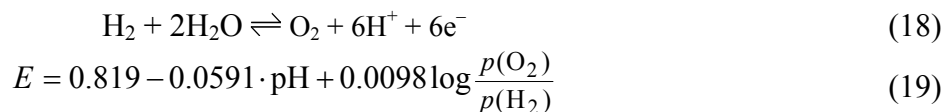






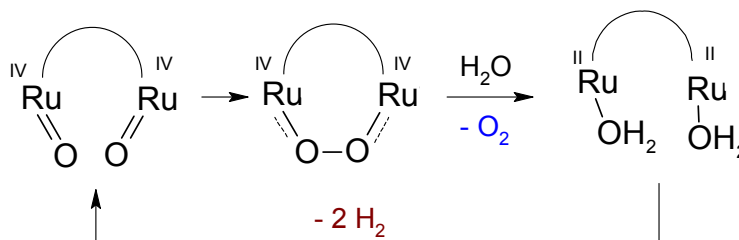


inhibited. The relative predominance of dissolved oxygen and hydrogen in water, within the electrochemical stability window of water, can be estimated by the formal reaction (18) at 25 °C [44]:



At potentials below  $E$ , dissolved hydrogen is thermodynamically stable in aqueous solutions; at potentials above  $E$  oxygen is predominant. In Figure 4-b, line 1 ( $\text{pH} > 7$ ) corresponds therefore to absorbed oxygen, and line 2 ( $\text{pH} < 7$ ) to absorbed hydrogen, which determine the cell voltage of the metal oxide-glassy carbon cell.

Recently, a mechanistic study and  $^{18}\text{O}$  labeling experiment on the photochemical oxidation of water at binuclear ruthenium complexes [45] illustrated the four oxidative electron-transfer process that takes the catalyst from its initial II,II oxidation state up to the formal IV,IV oxidation state. Once the Ru(IV) oxidation state is reached, two additional slower kinetic processes take place, corresponding to the formation of an intermediate that finally evolves oxygen. This result clarifies the intramolecular reaction pathway for the formation of the oxygen–oxygen bond in the case of adjacent ruthenium(IV) atoms.



**Cross sensitivity.** The proton exchange mechanism at a glass surface can basically be reproduced by platinum metal oxide-hydrates. However, the  $\text{RuO}_2$ -solution interface appears to be not a selective proton conductor, because its conductivity depends considerably on the ionic composition of the solution. In distilled water and phthalate buffer ( $\text{pH} 7$ ), quite different electrode potentials are measured at the metal oxide electrode due to the difference of *ionic strength*. Further problems are caused by the formation of ruthenium cluster ions, the sensitivity against other ions than  $\text{H}^+$ , and the type of the reference electrode.

The Nernst slope, which generally deviates from  $59 \text{ mV pH}^{-1}$  (25 °C), is nearly independent of dissolved anions in the solution (such as  $0.1 \text{ mol/L}$  of  $\text{SO}_4^{2-}$ ,  $\text{Br}^-$ ,  $\text{Cl}^-$ , and  $\text{NO}_3^-$ ). However, commercial  $\text{RuO}_2$  resistive pastes, which contain  $\text{PbO}$ , exhibit a slope which depends on different anions significantly [46].

Reducing agents (e.g. ascorbic acid,  $\text{Fe}^{2+}$ , sulfite) and oxidants ( $\text{H}_2\text{O}_2$ ,  $\text{I}^-$ ) damage the reversibility at both anodic and cathodic potentials, which reveals the role of adsorbed hydrogen and oxygen for the measured mixed potentials. Traces of platinum (being a recombination catalyst) significantly alter the cyclic voltammogram of a  $\text{RuO}_2$  electrode, especially in the hydrogen region.

**Preparation.** Since the 1980s, etched titanium sheets have been repeatedly dip-coated in an alcoholic solution of  $\text{RuCl}_3 \cdot 3\text{H}_2\text{O}$ , followed by drying and pyrolysis at  $300\text{--}350 \text{ °C}$  [47]. Higher

decomposition temperatures destroy the active surface area of the electrode, and yield less marked jumps of cell voltage in the acid-base titration curve at pH 7.

In the 1990s, it got evident that the specific capacitance at the electrode-electrolyte interface can be enhanced by a residual amount of water in the  $\text{RuO}_2 \cdot x\text{H}_2\text{O}$  material [48], which corresponds to the presence of Ru(III) in the disturbed rutile lattice. High surface area ruthenium oxide-hydrate;  $\text{RuO}_2 \cdot x\text{H}_2\text{O}$  [49], prepared by alkaline precipitation [50] from  $\text{RuCl}_3$  solutions at about pH 7.5 (sol-gel process [51]), washed several times with water, dried at 90 °C, and finely dispersed in a mixture of polyalcohols, can be screen-printed on carbon fiber paper or nickel supports [52]. Commercial  $\text{RuO}_2 \cdot x\text{H}_2\text{O}$  has a water content between  $x = 1$  and 3. Heat treating at 200 °C reduces the water content to  $x = 0.4$ , or 5% by weight.

The IR absorption of solid  $\text{RuO}_2$  powders, due to the stretch vibration of H-bridged OH-groups above  $3000 \text{ cm}^{-1}$ , is strongest for sol-gel  $\text{RuO}_2$ , whereas the thermally prepared powders contain less adsorbed or chemically bound water. In contrast to the “thermal” powders, the colloidal sol-gel  $\text{RuO}_2$  forms a considerable amount of coloured ions in aqueous solution, which appear to be important for redox capacitance. The SIMS spectra of sol-gel  $\text{RuO}_2$  reveal mass peaks at 133 u and 149 u, which might be attributed to the predominant Ru(III) and Ru(IV) species minus a proton, and cannot be found in single crystalline  $\text{RuO}_2$  in this significant amount [53].  $\text{RuO}_2$  electrodes under current age by partial oxidation of the surface sites, i.e. by a loss of Ru(III) surface sites, which are essential for the dissociative adsorption of water involving proton conductivity.

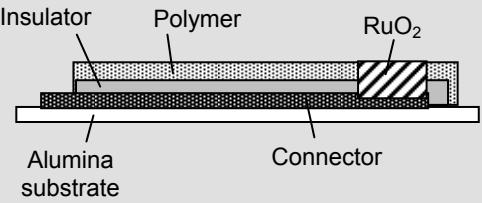
**Non-aqueous solutions.** The interfacial capacitance of platinum metal oxides in organic solutions is considerably lower than in aqueous solution.  $\text{RuO}_2$  typically contains a certain amount of residual water, which allows the development of an equilibrium potential based on the dissociative adsorption of water in non-aqueous solutions, too. Comprehensive information on this topic is not available in the literature.

#### 4.2. Applications of Ruthenium Dioxide Sensors

Usual thick film sensors are prepared by three inks or pastes which are screen-printed onto alumina: Ag-Pd paste as conductor, metal oxide paste as active surface and an overglaze paste as protector. In recent years, finely dispersed platinum metal oxides were coated on carbon particles or bound in polymers [54,55,56]. Polymer bound metal oxide electrodes can be fabricated by coating metal plates with a thin layer of a mixture of metal oxide powder in commercial varnish based resins. The best pH sensitivity is achieved by a mixture of 10% sol-gel  $\text{RuO}_2 \cdot x\text{H}_2\text{O}$  (water content  $\sim 7.2\%$ ) in a matrix of epoxy or polyester [57]. Reactive sputtering of platinum metal targets in argon-oxygen atmospheres is used to produce 1  $\mu\text{m}$  thick oxide electrodes on alumina and silicon substrates; palladium and platinum oxides were found to be less stable than ruthenium oxide [58]. An overview of applications [59] is given in Table 5. Both potentiometric and amperometric sensors [60] have been used.

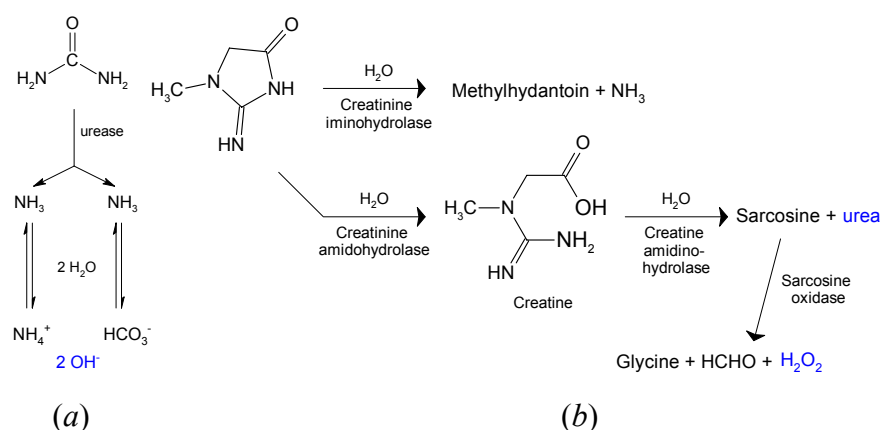


**Table 5.** Examples for pH sensors and measuring techniques based on RuO<sub>2</sub>.

Construction of the sensor: WE = working electrode, RE = reference, CE = counter	Applications and properties	Ref.
<p><i>Film layers</i> Screen-printed layers of graphite-based conducting inks containing 10% RuO<sub>2</sub></p>	<p>Lemonades, wine and milk. Sensitivity: <math>-51 \text{ mV pH}^{-1}</math> Response time: <math>&lt; 5 \text{ min}</math></p>	[61]
<p>Planar thick-film of RuO<sub>2</sub>·xH<sub>2</sub>O in a polymer matrix on a current collector on a alumina substrate</p>	<p>651 mV vs. Ag AgCl (pH 0) <math>-52 \text{ mV pH}^{-1}</math> (pH 2–10)</p>	[62]
<p>Thick-film fabricated chemical sensor: RuO<sub>2</sub> in a polymer binder on gold back contact.</p> 	<p>Application in water-based inks: Sensitivity: <math>-47 \text{ mV pH}^{-1}</math> (pH 4–10) pH sensitivity drift: <math>50 \mu\text{V pH}^{-1} \text{ d}^{-1}</math> Previous calibration is needed. Drift of thick-film Ag AgCl reference electrode: <math>dU/dpH = [-0.070 \ln(t/d) + 0.125] \text{ mV}</math></p>	[63]
<p><i>ISFET</i> RuO<sub>2</sub> sensing membrane on a <i>p</i>-type silicon wafer substrate by radio frequency sputtering (Ru metal, 1.3 Pa, in Ar/O<sub>2</sub>; 10 W, 13.56 MHz). Drain-source voltage 0.2 V; gate voltage <math>U_G = 0-6 \text{ V}</math>; while the drain-source current <math>I_{DS}</math> is measured.</p>	<p>Applications: lemonades, vinegar, milk, water. Sensitivity: <math>\sim 57 \pm 1 \text{ mV pH}^{-1}</math> (<math>I_{DS} = 200 \mu\text{A}</math>) Response time: <math>&lt; 1 \text{ s}</math> Drift rate: <math>0.13 \text{ mV pH}^{-1}</math> (pH 4) <math>0.38 \text{ mV pH}^{-1}</math> (pH 7) <math>7.31 \text{ mV pH}^{-1}</math> (pH 10), Hysteresis width: <math>4.4 \text{ mV}</math> (pH 7–4–7–10–7) <math>2.2 \text{ mV}</math> (pH 7–10–7–4–7) Loop time: <math>\sim 13 \text{ min}</math> Interfering ions: <math>\text{K}^+, \text{Na}^+</math> (<math>k \approx 4 \cdot 10^{-6}</math>, Equation 4) The <math>I_{DS}(U_G)</math> curve is shifted positively as the pH value increases (see Figure 3).</p>	[64]
<p><i>Coulometric micro-tritrator:</i> Actuator for the coulometric production: two gold electrodes (on copper support) End-point detection: Ru/RuO<sub>2</sub> (WE), Ag AgCl (RE), Au (CE)</p>	<p>Acid-base titration, e.g. 0.01 molar acetic acid: <math>\Delta E = \sim 200 \text{ mV}</math> at <math>6.8 \mu\text{A}</math> applied current</p>	[65]
<p><i>Amperometric Biosensor:</i> 5% Ru/carbon/enzyme (WE) on a silver-conductive layer (CE) on a polyester support</p>	<p>Pesticides monitoring by help of acetylcholine esterase and choline oxidase at 700 mV vs. SCE: Acetylcholine + H<sub>2</sub>O → Acetate + Choline Choline + O<sub>2</sub> → Betaine aldehyde + H<sub>2</sub>O<sub>2</sub> The measured current is proportional to choline concentration in phosphate buffer (pH 7).</p>	[66]
<p><i>Potentiometric biosensor:</i> RuO<sub>2</sub>/urease (WE) and RuO<sub>2</sub>/bovine serum albumin (CE) on silver current collector</p>	<p>Flow injection system: Dialysate fluid and buffer are continuously dropped on the sensor by help of a peristaltic pump.</p>	[67]
<p>59.5% RuO<sub>2</sub>, 40% graphite paste, 0.5% urease, screen-printed on a current collector.</p>	<p>Detection of silver and copper ions, which inhibit urease, by a change of potential: <math>\sim 50 \text{ mV mmol}^{-1}</math></p>	[68]

**Biosensors** [69,70,71]. Among a large variety of potentiometric sensors using biocatalytic and bioaffinity-based mechanisms, the detection of urea and creatinine is most advanced. Sensors based on RuO<sub>2</sub> and urease are in development for the determination of heavy metals, which inhibit the enzymatic hydrolysis of urea:  $\text{NH}_2\text{CONH}_2 + 3\text{H}_2\text{O} \rightarrow 2\text{NH}_4^+ + \text{HCO}_3^- + \text{OH}^-$  (Figure 5).

**Figure 5.** (a) Principle of the urea biosensor based on pH-measurements. By enzymatic hydrolysis, alkaline products are formed. (b) The creatinine sensor is based on the detection of consumed oxygen or produced hydrogen peroxide during the enzymatic conversion of the analyte.



The pH sensitive RuO<sub>2</sub> layer serves as a transducer for the ionic reaction products. On the RuO<sub>2</sub> electrode, screen-printed on ceramic substrate, urease in polyvinylchloride is adsorbed and then immobilized in a polymer such as Nafion. The biosensor can be cleaned from heavy metals by a solution of EDTA; a constant urea concentration is applied in a TRIS buffer, and the change of electrode potential (vs. Ag|AgCl) is observed after a given time due to the decreasing rate of substance conversion in the presence of heavy metal ions [72].

1. Label-based *immunosensors* contain antibodies as analyte recognition parts. Horseradish peroxidase and alkaline phosphatase, e.g., catalyze reactions which produce electroactive products in immunoenzymatic biodevices. For example, at a polypyrrole coated screen-printed gold electrode, peroxidase may work as biocatalytic label converting *o*-phenylene-diamine into 2,3-diaminophenazine (in the presence of H<sub>2</sub>O<sub>2</sub>). Label-based analytical sensors with enzymatic, fluorescent, radiochemical, and nanoparticle markers rely on amperometric and optical detection rather than on potentiometry.

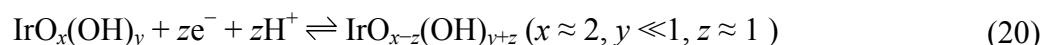
2. Label-free *bioaffinity sensors* were realized by the aid of protein coated ISFETs, which dynamically measure the release or uptake of protons by biologically active protein molecules bound on the semiconductor. Antibodies can be adsorbed on colloidal nanoparticles (Au, Ag) in a polymer matrix (e.g. gelatin, nafion, polyvinyl butaral, thiosilane gel, poly(*o*-phenylenediamine)) on a metal support. Potentiometric genosensors – as field effect devices or membrane ion-selective electrodes, modified with oligonucleotides – shall detect complementary DNA sequences.

Although the biorecognition is mostly specific, the generation of the potentiometric signal remains unclear, and are strongly affected the composition of the analysed samples. Biosensors based on voltammetry, piezoelectricity, or optical spectroscopy seem more promising for practical applications.

### 4.3. Iridium Dioxide

IrO<sub>2</sub> [73] promises to be a superior material for pH measurements in technical media, such as fuels [74], food applications [75], and in biological media [76]. Iridium oxide provides: (i) a wide linear pH response range, with negligible interference of ions and complexing agents, (ii) a fast and stable response in aqueous, nonaqueous, non-conductive, and even corrosive media, (iii) high conductivity, low temperature coefficient, and no requirement for pretreatment.

**Redox chemistry.** In air-saturated solutions, iridium is covered by adsorbed oxygen atoms, which take part in redox reactions involving hydrogen ions. Anodic oxidation or heating in an oxygen atmosphere creates a surface layer of IrO<sub>2</sub> with improved redox properties. The anodic and cathodic peaks in the cyclic voltammogram of an IrO<sub>2</sub> electrode are attributed to the Ir<sup>IV</sup>/Ir<sup>III</sup> redox transition, which is accompanied by the release and uptake of protons. During potential cycling of an iridium wire, the Ir<sup>IV</sup>/Ir<sup>III</sup> transition becomes less reversible at high scan rates, resulting in the growing IrO<sub>2</sub> layer; the net cathodic current is smaller than the net anodic current:



Electrodes prepared by thermal decomposition of iridium chloride or H<sub>2</sub>IrCl<sub>6</sub> on a titanium support, as well as sputtered IrO<sub>2</sub> on stainless steel and tantalum, respond to pH with a Nernstian sensitivity of nearby 59 mV/pH; whereas anodically prepared films exhibit a super-Nernstian response between 62 and 77 mV/pH [77]. The dU/dpH slope drops with time, because the oxide hydration changes. The apparent electrode potential, obtained by extrapolating to pH 0, is close to the calculated value reported by POURBAIX for the reaction 2IrO<sub>2</sub> + 2H<sup>+</sup> + 2e<sup>-</sup> ⇌ Ir<sub>2</sub>O<sub>3</sub> + H<sub>2</sub>O, namely E<sup>0</sup> = 926 mV vs. NHE (682 mV vs. SCE). However, during aging over a 60 days period, the electrode potential decreases by roughly 150 mV from the initial value for a freshly prepared electrode.

**Preparation.** IrO<sub>2</sub> electrodes have been prepared by (i) thermal decomposition of iridium salts, (ii) sol-gel processes, (iii) electrochemical or thermal oxidation of iridium wires, e.g. continuous potential cycling in aerated H<sub>2</sub>SO<sub>4</sub> solution for several hours; (iv) reactive r.f. sputtering from a metallic iridium target in an oxygen plasma, (v) pulsed-laser ablation of iridium oxide targets; (vi) anodic, cathodic or electrophoretic deposition. In a polymer matrix, e.g. in Nafion [78] or PTFE-bound graphite [79], IrO<sub>2</sub> can be employed as a planar thick-film pH sensor using an interdigital structure [80] of the current collectors, e.g. of silver [81].

Potentiometric solid-state sensors are claimed to be rugged, and reference solutions are not needed [82], if the pH-sensitive working electrode is an iridium wire that has been partially oxidized to IrO<sub>2</sub> (about 15 μm thick). The counter-reference electrode may be nearby pH-insensitive rhodium foil that is covered by a 5 μm thick rhodium oxide layer. The potential difference declines approximately linear in the range between pH 2 to pH 12. The slope of about -30 mV/pH is coined by the Rh/RhO<sub>2</sub> electrode (-26 mV/pH), whereas the Ir/IrO<sub>2</sub> electrode shows Nernstian behaviour (-58 mV/pH).

**Cross sensitivity** [83,84]. Metal cations ( $\text{Fe}^{3+}$ ,  $\text{Fe}^{2+}$ ,  $\text{Pb}^{2+}$ ,  $\text{Cu}^{2+}$ ,  $\text{Ag}^+$ ) cause a small shift of some millivolts in the potential-pH response of the  $\text{IrO}_2$  electrode;  $\text{Ni}^{2+}$ , and dissolved oxygen cause a shift of some ten millivolts. The addition of sulfate, sulfite, borate, phosphate, and ammonia to the electrolyte causes no detrimental effects; whereas oxalate, iodide, bromide, disulfite, thiosulfate,  $[\text{Fe}(\text{CN})_6]^{3-}$  and  $[\text{Fe}(\text{CN})_6]^{4-}$  alter the characteristics of the electrode more or less slightly and irreversibly.

**Stability and recycling** [85].  $\text{IrO}_2$  films can be removed from electrode supports by (i) aqua regia, (ii) anodic dissolution in 2 M  $\text{H}_2\text{SO}_4$ ; or (iii) applying successive potentials of  $-3.0$  V and  $+2.5$  V (vs.  $\text{Ag}|\text{AgCl}$ ) in 0.3 M  $\text{Na}_2\text{HPO}_4$  solution.

## 5. Tin Dioxide and Lead Dioxide

The electrical conductor  $\text{SnO}_2$  [86,87] can be deposited on indium tin oxide glass (ITO) by sputtering [88]; it shows a much narrower dynamic range than the pH glass electrode; the Nernst slope equals about  $-58$  mV/pH (pH 2 – 12). Commercial doped  $\text{SnO}_2$  (49 mV/pH) works mainly as a redox electrode. The sensing area, i. e. the length of the pH-sensitive tip of the glass micro electrode, should not be less than about  $4$  mm<sup>2</sup> in order to avoid a critical reduction of the pH response ( $\ll 59$  mV pH<sup>-1</sup>). Sputtering of suitable  $\text{IrO}_2$  films succeeds best at 20%  $\text{O}_2$  gas, and a pressure of 2.7 Pa (0,02 Torr).

$\text{PbO}_2$  was recognized a pH probe already in the 1970s; it can be deposited on titanium and aluminium supports [89]. The electrode potential vs. saturated calomel (SCE) decreases linearly according to the reaction  $\text{PbO}_2 + \text{H}^+ + \text{e}^- \rightarrow \text{PbO}(\text{OH})$ . Anions alter the electrode potential slightly ( $<5\%$  at pH 7 in 1-millimolar solution of nitrate, hydrogencarbonate, phosphate, citrate), whereas cations (1 mmol/L of  $\text{Li}^+$ ,  $\text{Na}^+$ ,  $\text{Mg}^{2+}$ ,  $\text{Ca}^{2+}$ ,  $\text{NH}_4^+$ ) have no adverse effect. The interference of  $\text{NH}_4^+$  is marked in alkaline solutions.

## 8. Transition Metal Oxides

$\text{TiO}_2$  and mixed  $\text{TiO}_2/\text{RuO}_2$  [90,91],  $\text{Ta}_2\text{O}_5$ ,  $\text{WO}_3$ ,  $\text{MnO}_2$  [92],  $\text{RhO}_2$ ,  $\text{OsO}_2$ ,  $\text{PdO}$  [93], molybdenum bronzes and other oxides and have been described as materials for pH sensors in literature. Most oxides are useful between pH 2 to pH 11, and show a pronounced hysteresis, i. e. the electrode potential suffers a shift if the solution changes from pH 2 to pH 12, and back to pH 2 again.  $\text{RuO}_2$  and  $\text{OsO}_2$  show good accuracy ( $\pm 2$  mV).  $\text{Ta}_2\text{O}_5$  behaves poor in a carbon-bound electrode ( $\pm 30$  mV).

pH-sensors based on  $\text{ZrO}_2$  and  $\text{Y}_2\text{O}_3/\text{ZrO}_2$  (YSZ) for pH measurements under high pressure are mentioned in the literature [94,95,96].

## 9. Non-Oxidic Materials and Support Materials

Aluminiumnitride (AlN) [97] and Galliumnitride (GaN) have been described for a  $\text{H}^+$  ion-sensitive field-effect transistor (ISFET).

*Conducting polymers* such as polypyrrole, polyaniline, and the proton conductor Nafion were described for solid-state pH sensors.

Activated carbon and soot contain some percent of oxygen, typically bound in acidic or basic surface groups, which allow ion exchange with the surrounding solution. The quasi-stationary potential of a polymer-bound activated carbon electrode on an aluminium support, supplied by GORE for use in supercapacitors, is shown in Figure 6. Between pH 6 and pH 9, the electrode could be used as a quasi-reference electrode in aqueous solution.

Indium oxide in a matrix of epoxy resin on etched aluminium foil [98] extends the range of nearby constant potential range from pH 5 to pH 11. The material might be interesting for a novel reference system (see Section 7).

## :. Reference Electrodes

The experimental conditions of the standard hydrogen electrode (SHE) [99] are all but trivial to fulfil. The most stable calomel electrode ( $\text{Hg}|\text{Hg}_2\text{Cl}_2|\text{Cl}^-$ ) is no longer used due to environmental concerns and the toxicity of mercury. Therefore, usually the  $\text{Ag}|\text{AgCl}|\text{KCl}$  (3.5 mol/L) reference electrode is used for chemical sensors [100, 101]. The liquid filling, however, complicates miniaturisation and applications at higher pressures and temperatures.

*Silver-silver chloride electrode.* The  $\text{Ag}|\text{AgCl}|\text{Cl}^-$  electrode works basically without any AgCl on its surface; AgCl can be dispersed in the solution, but the response to the chloride ions is slow according to the equilibrium:  $\text{Ag}^+_{(s)} + \text{Cl}^-_{(s)} \rightleftharpoons \text{AgCl}_{(s)}$ .

**Figure 6.** (a) Quasi-stationary pH response of plain electrodes after 10 mins at 21 °C. Size: 10x10 mm. (b) Impedance spectra of an  $\text{In}_2\text{O}_3/\text{WO}_3$  electrode (polymer-bound mixture on active carbon support) in buffer solutions at 20 °C. Reference electrode:  $\text{Ag}|\text{AgCl}|\text{KCl}$ , counter electrode: platinum [100].

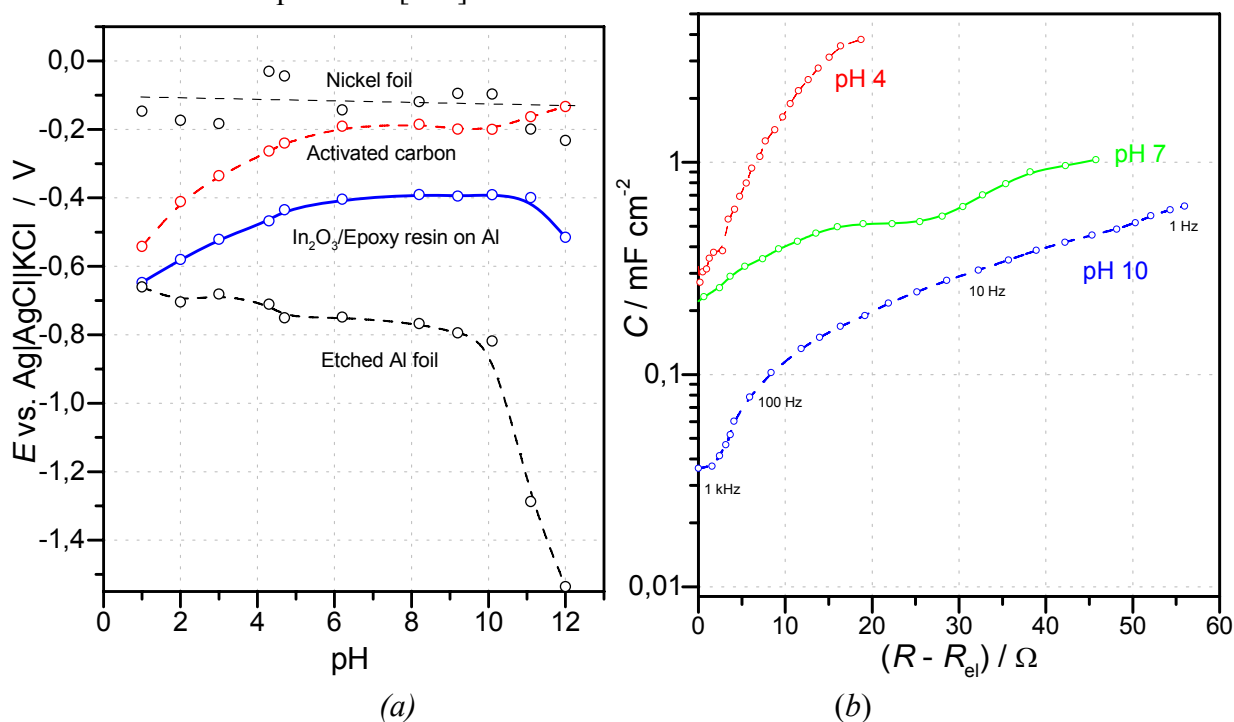
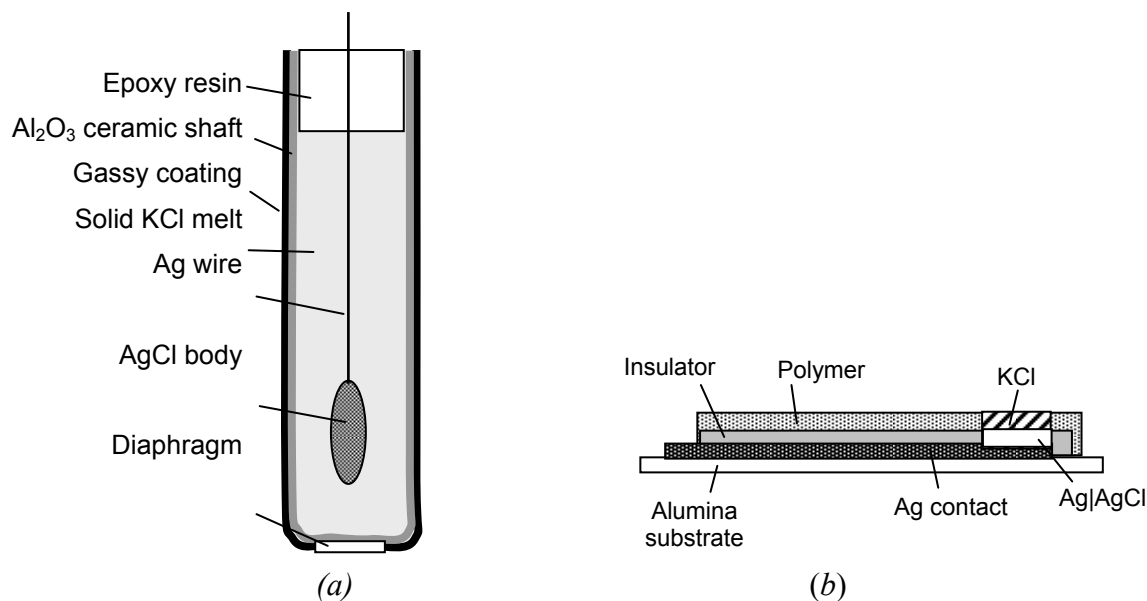


**Figure 7.** (a) Principle of an all-solid-state reference electrode after Meinsberg Kurt-Schwabe Research Institute. (b) Thick film silver-silver chloride reference electrode [102].



- At a porous AgCl coating in direct contact to the solution, redox reactions (e.g.  $O_2/OH^-$ ) cause a mixed potential which deviates from the ideal response (+ 202 mV vs. SHE in sat. KCl solution, 20–25 °C). AgCl is a silver ion conductor. Voltage stability can be improved by small grains, and a thermal treatment of the AgCl coating below 455 °C [103]. As the chloride electrolyte is necessary, the  $Ag|AgCl|Cl^-$  electrode requires a liquid junction across a diaphragm. All-solid electrodes for sensors are shown in Figure 7.
- *Gel-like electrolytes* are useful at temperatures up to 140 °C and pressures up to 15 bar, however, at cost of increased diffusion potentials, irreversible bleeding, biofouling and aging of the gel.  $Ag|AgCl$  on a flat support material can be coated by a hydrogel (e.g. polyacrylamide) and surrounded by a membrane. The long-term stability of such reference electrodes in ISFETs is poor.
- *Polymer-electrolyte* reference systems (e.g. solid KCl in polyester resin) and open junctions are commercially available, e.g., under the brand name XEROLYT<sup>®</sup>.
- *All-solid-state* reference electrodes [104] would be most favourable. In a cylindrical shaft of porous alumina ceramic, which additionally serves as a diaphragm for the liquid junction, molten KCl is filled around a centered  $Ag|AgCl$  electrode [105]. AgCl diffuses partly in the KCl phase. Humidity from the environment provides the necessary conductivity in the hygroscopic KCl phase.
- Thickfilms of *noble metal filled glass* (e.g. Corning 015) on oxide ceramic or steel supports show increased resistivity, response times in the range of minutes, and relatively short lifetime. The reference potential does often not obey the Nernst slope. Different thermal expansion coefficients between glass and ceramic support cause cracks.
- The impact of a *glassy carbon* rod electrode under ambient conditions and the presence of dissolved oxygen, is shown in Figure 4-b. A linear function of cell voltage in the range between pH 2 to pH 12 was obtained by use of a plane gold counter-reference electrode; the total

capacitance of the cell is dominated by the large capacitance of the rough RuO<sub>2</sub> electrode,  $C = [C_{\text{RuO}_2}^{-1} + C_{\text{Au}}^{-1}]^{-1} \approx C_{\text{RuO}_2}$ . Gold is known as an electrode material with negligible hydrogen sorption; the oxygen overpotential is higher than that of platinum.

- Rhodium foil, that is covered by a rhodium oxide layer, behaves nearby pH-insensitive (see Section 4.3).
- Molybdenum and tungsten bronzes [106], e.g. Li<sub>0.4</sub>Mo<sub>0.95</sub>W<sub>0.05</sub>O<sub>3</sub> [107] do not significantly respond to pH changes, oxygen concentration and redox potential of the solution. However, they are sensitive to alkali ions ( $\text{K}^+ < \text{Na}^+ < \text{Li}^+$ ), but the preparation of single-crystalline electrodes is hardly reproducible.
- Manganese dioxide, H<sub>x</sub>MnO<sub>2</sub> [108], suffers from poor reproducibility.
- Boron carbide might be useful as electrode material having a high hydrogen overvoltage.
- Prussian Blue as a reference in all-solid state pH glass electrodes was investigated in [109].

### ; . Measuring Techniques

Traditionally, the potentiometric method is favoured for pH measurements. Additionally, amperometry has been established especially for biosensors (see Table 5). The coulometric determination of proton concentrations offers for future sensor applications, e.g. based on redox active metal oxides. However, much work has to be done to finally correlate the faradaic redox reactions, which directly depend on pH, from all capacitive surface effects which reflect the electrolyte-electrode interface and the composition of the surrounding solution.

As a preliminary step to a future direct recording pH sensor, *ac* impedance spectroscopy [110] might be useful. This technique allows the separation of electrolyte resistance, charge transfer processes and diffusion processes along the grain-boundaries and in the three-dimensional pores of the material. Tungsten trioxide, in a mixture with indium oxide [100] is shown in Figure 6 for use in a capacitive pH sensor. The solution resistance  $R_{\text{el}}$  is subtracted from the measured impedance to exclude both the geometric dimensions of the sensor and the ionic conductivity of the solution. Then the frequency-dependent interfacial capacitance  $C_{\text{p}}(\omega)$ , corrected by the solution resistance, is calculated for each frequency  $f$  from the measured real and imaginary parts according to Equation 22.

$$C_{\text{p}}(\omega) = \frac{-\text{Im}Z}{2\pi f[(\text{Re}Z - R_{\text{el}})^2 - (\text{Im}Z)^2]} \quad (22)$$

If the *dc* resistance  $R$  of the pH measuring cell is assumed to be large, it holds  $C_{\text{S}}(\omega) = [2\pi f \text{Im} Z]^{-1} \approx C_{\text{P}}$  at low frequencies. Then the parallel equivalent circuit  $R_{\text{el}}-C_{\text{P}}||R_{\text{P}}$  simplifies to a series combination, of  $R_{\text{el}}-C_{\text{S}}$ . Both  $C_{\text{P}}$  and  $C_{\text{S}}$  are frequency-dependent differential capacitances. The pH sensor may work either at a given frequency or differential capacitance is averaged by integration in a given frequency range. The change of resistance and capacitance may also be used in commercial pH meters as a diagnostic tool for the aging of a pH electrode and the requirement for re-calibration [111].

## 10. Conclusions

1. A common reference system valid for pH measurements in all media is still missing; as well, there is no simple pH reference besides the intricate standard hydrogen electrode and the Harned cell. The pH values in non-aqueous solutions cannot simply be compared with those in aqueous systems. A coulometric proton titrator might be the solution for this problem, once appropriate directly pH dependent materials are known.

2. For the potentiometric pH determination in aqueous solutions, the glass electrode is still unsurpassed. For special applications in solutions containing fluoride or alkali, metal oxide electrodes have been introduced; whereby the antimony electrode is the most prominent example.

3. The electrode-electrolyte interface at platinum metal oxides is able to exchange protons with the surrounding solution. RuO<sub>2</sub> and IrO<sub>2</sub> were successfully applied for disposable applications in technical solutions and biological media. ISFETs based on platinum metal oxides suffer from poor long-term stability yet.

4. The redox pseudocapacitance of hydrous RuO<sub>2</sub>, in which protons are involved, is considered as a model system. Relative pH measurements based on standard buffer solutions are already possible by impedance spectroscopy. For absolute pH determination, the separation of interfacial surface charges and faradaic charges has still to be solved.

5. Platinum metal oxides can easily be coated on nickel foil by thermal decomposition of precursor solutions. Powders, e.g. obtained by sol-gel processes, can be bound in an epoxy matrix.

6. Activated carbon, glassy carbon, and possibly indium oxide seem to be useful as liquid-free reference systems in pH sensors at values between pH 5 and pH 10.

## Symbols and Abbreviations

<i>a</i>	activity, $a = \gamma_c(c/c^0) = \gamma_m(m/m^0)$
<i>C</i>	capacitance (F), $C = dQ/dU$
<i>c</i>	molar concentration (mol/L), amount of a substance solved per liter of solution
<i>c</i> <sup>0</sup>	standard concentration: $c^0 \equiv 1 \text{ mol/L}$
CE	counter electrode
CVD	chemical vapour deposition
<i>E</i>	potential of an electrode versus a reference electrode (in V vs. ref)
<i>E</i> <sup>0</sup>	standard potential of an electrode or half-reaction (V NHE): at 25 °C, 101325 Pa, 1-active solution
$\Delta E^0$	difference in standard potential of two half-cells (V), electromotive force
<i>F</i>	Faraday constant; charge on one mole of electrons: $F = 96485 \text{ C mol}^{-1}$
<i>I</i>	electric current (A)
<i>j</i>	imaginary operator, $\sqrt{-1}$
<i>Q</i>	electric charge (C = A s)
<i>M</i>	molar mass of a compound ( $\text{kg mol}^{-1}$ )
<i>m</i>	molality ( $\text{mol kg}^{-1}$ ), amount of substance solved per kilogram of solvent: $m = c/(\rho - Mc)$
<i>m</i> <sup>0</sup>	standard molality: $m^0 \equiv 1 \text{ mol kg}^{-1}$



NHE	standard hydrogen electrode, see Section 2.2
$p$	pressure (1 Pa = 10 <sup>-5</sup> bar)
$p^0$	standard pressure: 101325 Pa
$R$	electric resistance ( $\Omega$ )
Ref	Reference (electrode)
RE	reference electrode
RHE	reversible hydrogen electrode: $E_{\text{NHE}} = E_{\text{RHE}} - 0.05916\text{pH}$ (25 °C)
(s)	solid phase
SCE	saturated calomel electrode
SHE	standard hydrogen electrode, see Section 2.2
$T$	absolute temperature (in K)
TRIS	tris(hydroxymethyl) aminomethane
$U$	electric voltage (V), potential difference between two electrodes
$\Delta\phi$	electric potential difference between two phases (V)
$\rho$	density of a liquid (1 kg m <sup>-3</sup> = 1 g/L = 0.001 g cm <sup>-3</sup> )
$v$	scan rate, $v = dU/dt$ (in V s <sup>-1</sup> )
WE	working electrode
$Z$	$ac$ impedance ( $\Omega$ ): $\underline{Z} = \text{Re } \underline{Z} + j \text{Im } \underline{Z}$
$z$	charge number of an ion; number of electrons transferred in the half-reaction equation
$\gamma$	activity coefficient

## References and Notes

1. Sørensen, S.P.L.; Linderstrøm-Lang, K. The determination and value of pH. *Comp. Rend. Trav. Lab. Carlsberg* **1909**, *8*, 1-168.
2. Vonau, W.; Guth, U. pH monitoring: A review. *J. Solid State Electrochem.* **2006**, *10*, 746-752.
3. Bates, R.G. *Electrometric pH-Determinations, Theory and Practice*; John Wiley and Sons: New York, NY, USA, 1954.
4. Haber, F.; Klemensiewicz, Z. Ueber elektrische Phasengrenzkräfte. *Zeitschr. f. Physik. Chem.* **1909**, *67*, 385-431.
5. Galster, H. *pH Measurements.—Fundamentals, Methods, Applications, Instruments*; VCH Publishers: New York, NY, USA, 1991.
6. *Ion Selective Electrodes*, Koryta, J., Stulik, K., Eds.; Cambridge Univ. Press: Cambridge, UK, 1983.
7. Covington, A.K.; Bates, R.G.; Durst, R.A. Definition of pH scales, standard reference values, measurement of pH, and related terminology (IUPAC Recommendations 1984). *Pure Appl. Chem.* **1985**, *57*, 531-542.
8. Janata, J. *Principles of Chemical Sensors*; Plenum Press: New York, NY, USA, 1989.
9. *Glass Electrodes for Hydrogen and Other Cations*, Eisenman, G., Ed.; Marcel Dekker: New York, NY, USA, 1967.

10. Covington, A.K.; Büttikofer, H.P.; Camoes M.F.G.F.C.; Ferra, M.I.A.; Rebelo, M.J.F. Procedures for testing pH-responsive glass electrodes at 25, 37, 65 and 85 °C and determination of alkaline errors up to 1 mol/dm<sup>3</sup> Na<sup>+</sup>, K<sup>+</sup>, Li<sup>+</sup> (IUPAC Technical Report). *Pure Appl. Chem.* **1985**, *57*, 887-898.
11. Harned, H.S.; Owen, B.B. *The Physical Chemistry of Electrolytic Solutions*; Reinhold: New York, NY, USA, 1958; Chap. 14.
12. Buck, R.P.; Rondinini, S.; Covington, A.K.; Baucke, F.G.K.; Brett, C.M.A.; Camoes, M.F.; Milton, M.J.T.; Mussini, T.; Naumann, R.; Pratt, K.W.; Spitzer, P.; Wilson, G.S. Measurement of pH. Definitions, standards, and procedures (IUPAC Recommendations 2002). *Pure Appl. Chem.* **2002**, *74*, 2169-2200.
13. Rondinini, S.; Mussini, P.R.; Mussini, T.; Vertova, A. pH measurements in non-aqueous and mixed solvents: predicting pH(PS) of potassium hydrogen phthalate for alcohol-water mixtures (IUPAC Technical Report). *Pure Appl. Chem.* **1998**, *70*, 1419-1422.
14. Kortüm, G. *Lehrbuch der Elektrochemie*. Verlag Chemie: Weinheim, Germany, 1970; Chap. XI.2.
15. Kratz, L. *Die Glaselektrode und ihre Anwendungen*, D. Steinkopff: Frankfurt, Germany, 1950; pp. 199-200.
16. Bergveld, P. Development of an ion-sensitive solid state device for neurophysiological measurements. *IEEE Trans. Biomed. Eng.* **1970**, *BME-17*, 70-71.
17. *Sensors. A Comprehensive Survey*, Göpel, W., Hesse, J., Zemel, J.N., Eds.; VCH Publisher: Weinheim, Germany, 1991; Vol. 2.
18. Abe, H.; Esahi, M.; Matsuo, T. ISFET's using inorganic gate thin films. *IEEE Trans. Electron Devices* **1979**, *ED-26*, 1939-1944.
19. Liao Y-H.; Chou, J.-C. Preparation and characteristics of ruthenium dioxide for pH array sensors with real-time measurement system. *Sens. Actuat. B* **2008**, *128*, 603-612.
20. Manufacturer: Pfaudler Werke AG, Schwetzingen, Germany.
21. Oesch, U.; Ammann, D.; Brzózka, Z.; Pham, H.V.; Pretsch, E.; Rusterholz, B.; Simon, W.; Suter, G.; Iti, D. H.; Xu, A.P. Design of neutral hydrogen ion carriers for solvent polymeric membrane electrodes of selected pH range. *Anal. Chem.* **1986**, *58*, 2285-2289.
22. *Manufacturer: Orion Research*; Cambridge, MA 02139, USA.
23. *Sensors Update*, Göpel, W., Baltes, H., Hesse, J., Eds.; VCH Publication: Weinheim, Germany, 2001; Vol. 8, Chap. 1.3.
24. *Sensoren*, Schaumburg, H., Ed.; Teubner: Stuttgart, Germany, 1992.
25. Biilmann, E. L'electrode à quinhydrone et ses applications. *Bull. Soc. Chim. France* **1927**, *41*, 213-286.
26. Kolthoff, I.M.; Hartong, B.D. On the antimony electrode. *Rec. Trav. Chim.* **1925**, *44*, 113-120.
27. Uhl, A.; Kestranek, Electrometric titration of acids and bases with an antimony indicator electrode. *Monatsh. Chem.* **1923**, *44*, 29-34.
28. Schwabe, K. Die Wismutelektrode zur pH-Indikation. *Z. Elektrochem.* **1951**, *55*, 411.

29. *Sensors. A Comprehensive Survey*, Göpel, W., Hesse, J.; Zemel, J.N., Eds.; VCH Publisher: Weinheim, Germany, 1991; Vol. 2.
30. Liu, J.H.; Zhang, Y.H.; Zhang, Z.Y.; Ni, L.; Li, H.X. Study of thick-film pH sensors. *Sens. Actuat. B* **1993**, *14*, 566-567.
31. Trasatti, S.; Lodi, G. *Conductive Metal Oxides*; Elsevier: Amsterdam, The Netherlands, 1980; Vol. A.
32. Beer, H.B. The invention and industrial development of metal anodes. *J. Electrochem. Soc.* **1980**, *127*, 303C.
33. Fog, A.; Buck, R.P. Electronic semiconducting oxides as pH sensors. *Sens. Actuat.* **1984**, *5*, 137-146.
34. Olthuis, W.; Robben, M.A.; Bergveld, P.; Bos, M.; van der Linden, W.E. pH sensor properties of electrochemically grown iridium oxide. *Sens. Actuat. B* **1990**, *2*, 247-256.
35. Ardizzone, S.; Daggetti, A.; Franceschi, L.; Trasatti, S. The point of zero charge of hydrous RuO<sub>2</sub>. *Colloids Surf.* **1989**, *35*, 85-96.
36. Trasatti, S. Physical electrochemistry of ceramic oxides. *Electrochim. Acta* **1991**, *36*, 225-241.
37. Trasatti, S.; Kurzweil, P. Electrochemical supercapacitors as versatile energy stores. *Platinum Met. Rev.* **1994**, *38*, 46-56.
38. Kurzweil, P. Electrochemical Capacitors. Metal Oxide. In *Encyclopedia of Electrochemical Power Sources*, Garche, J., Ed.; Elsevier: Amsterdam, The Netherlands, 2009.
39. Pourbaix, M. *Atlas of Electrochemical Equilibria in Aqueous Solutions*; NACE-Cebelcor: Brussels, Belgium, 1974.
40. Kurzweil, P. Precious metal oxides for electrochemical energy converters: Pseudocapitance and pH dependence of redox processes. *J. Power Sources* **2009**, *190*, 189-200.
41. Conway, B.E. *Electrochemical Supercapacitors*; Kluwer Academic/Plenum Publishers: New York, NY, USA, 1999; Chap. 11.
42. Doblhofer, K.; Metikos, M.; Ogumi, Z.; Gerischer, H. Electrochemical oxidation and reduction of the RuO<sub>2</sub>/Ti electrode surface. *Ber. Bunsenges. Phys. Chem.* **1978**, *82*, 1046-50.
43. Patel, A.; Richens, D.T. The tetranuclear ruthenium(IV) aqua ion: evidence in support of its formulation as H<sub>n</sub>[Ru<sub>4</sub>O<sub>6</sub>(OH<sub>2</sub>)<sub>12</sub>]<sup>(4+n)+</sup> (n = 0-4). *Inorg. Chem.* **1991**, *30*, 3789-3792.
44. Pourbaix, M. *Atlas of electrochemical equilibria in aqueous solutions*; NACE-Cebelcor: Brussels, Belgium, 1974.
45. Romain, S.; Bozoglian, F.; Sala, X.; Llobet, A. Oxygen-oxygen bond formation by the Ru-Hbpp water oxidation catalyst occurs solely via an intramolecular reaction pathway. *J. Am. Chem. Soc.* **2009**, *131*, 2768-2769.
46. Soto, J.; Labrador, R.H.; Marcos, M.D.; Martinez-Manez, R.; Coll, C.; Garcia-Breijo, E.; Gil, L. A model for the assessment of interfering processes in Faradic electrodes. *Sens. Actuat. A* **2008**, *142*, 56-60.
47. Sarangapani, S.; Lessner, P.; Forchione, J.; Griffith, A.; Laconti, A.B. Advanced double layer capacitors. *J. Power Sources* **1990**, *29*, 355-364.

48. Roginskaya, Y.E.; Morozova, O.V. The role of hydrated oxides in formation and structure of DSA-type oxide electrocatalysts. *Electrochim. Acta* **1995**, *40*, 817-822.
49. Mihell, J.A.; Atkinson, J.K. Planar thick-film pH electrodes based on ruthenium dioxide hydrate. *Sens. Actuat. B* **1998**, *48*, 505-511.
50. Wöhler, L.; Balz, P.; Metz, L. Die oxyde des rutheniums. *Z. Anorg. Allgem. Chem.* **1924**, *139*, 205-219.
51. Armelao, L.; Barreca, D.; Moraru, B. A molecular approach to RuO<sub>2</sub>-based thin films: sol-gel synthesis and characterization. *J. Non-Cryst. Solids* **2003**, *316*, 364-371.
52. Kurzweil, P. Long time stable electrode. *European patent EP 0622815, DE 4313474*, 1994.
53. Kurzweil, P. Precious metal oxides for electrochemical energy converters: Pseudocapacitance and pH dependence of redox processes. *J. Power Sources* **2009**, *190*, 189-200.
54. Takasu, Y.; Onoue, S.; Kameyama, K.; Murakami, Y.; Yahikozawa, K. Preparation of ultrafine RuO<sub>2</sub>-IrO<sub>2</sub>-TiO<sub>2</sub> oxide particles by a sol-gel process. *Electrochim. Acta* **1994**, *39*, 1993-1997.
55. Kim, H.; Popov, B.N. Characterization of hydrous ruthenium oxide/carbon nanocomposite supercapacitors prepared by a colloidal method. *J. Power Sources* **2002**, *104*, 52-61.
56. Jang, J.H.; Kato, A.; Machida, K.; Naoi, K. Supercapacitor performance of hydrous ruthenium oxide electrodes prepared by electrophoretic deposition. *J. Electrochem. Soc.* **2006**, *153*, A321-A328.
57. Kurzweil, P. Unpublished results, University of Applied Sciences: Amberg, Germany, 2009.
58. Kreider, K.G.; Tarlov, M.J.; Cline, J.P. Sputtered thin-film pH electrodes of platinum, palladium, ruthenium, and iridium oxides. *Sens. Actuat. B* **1995**, *28*, 167-172.
59. Vonau, W.; Enseleit, U.; Gerlach, F.; Herrmann, S. Conceptions, materials, processing technologies and fields of application for miniaturized electrochemical sensors with planar membranes. *Electrochim. Acta* **2004**, *49*, 3745-3750.
60. Allen, M.D.; Livesley, D.J.; Potter, R.J.; Pratt, A.S. (JohnsonMatthey) pH-meter with constant current applied between the transition metal-based sensor electrode and the reference electrode. *Patent WO/2000/004379*, 2000.
61. Koncki, R.; Mascini M. Screen-printed ruthenium dioxide electrodes for pH measurements. *Anal. Chim. Acta* **1997**, *351*, 143-149.
62. Mihell, J.A.; Atkinson, J.K. Planar thick-film pH electrodes based on ruthenium hydrate. *Sens. Actuat. B* **1998**, *48*, 505-511.
63. Gac, A.; Atkinson, J.K.; Zhang, Z.; Sion, R.P. A comparison of thick-film chemical sensor characteristics in laboratory and on-line industrial process applications. *Meas. Sci. Technol.* **2002**, *13*, 2062-2073.
64. Liao Y-H.; Chou, J.-C. Preparation and characteristics of ruthenium dioxide for pH array sensors with real-time measurement system. *Sens. Actuat. B* **2008**, *128*, 603-612.
65. Colombo, C.; Kappes, T.; Hauser, P.C. Coulometric micro-titrator with a ruthenium dioxide pH-electrode. *Anal. Chim. Acta*, **2000**, *412*, 69-75.
66. Cagnini A.; Palchettia, I.; Liontia, I.; Mascinia M.; Turnerbet A.P.F. Disposable ruthenized screen-printed biosensors for pesticides monitoring. *Sens. Actuat. B* **1995**, *24*, 85-89.

67. Tymecki, L.; Koncki, R. Thick-film potentiometric biosensor for bloodless monitoring of hemodialysis. *Sens. Actuat. B* **2006**, *113*, 782-786.
68. Ogonczyk, D.; Tymecki, L.; Wyzkiewicz, I.; Koncki, R.; Glab, S. Screen-printed disposable urease-based biosensors for inhibitive detection of heavy metal ions. *Sens. Actuat. B* **2005**, *106*, 450-454.
69. Thevenot, D.R.; Toth, K.; Durst, R.A.; Wilson, G.S. Electrochemical biosensors: recommended definitions and classification (IUPAC Technical Report). *Pure Appl. Chem.* **1999**, *71*, 2333-2348.
70. Koncki, R. Recent developments in potentiometric biosensors for biomedical analysis. *Anal. Chim. Acta* **2007**, *599*, 7-15.
71. Kotzian, P.; Brazdilova, P.; Kalcher, K.; Handlir, K.; Vytras, K. Oxides of platinum metal group as potential catalysts in carbonaceous amperometric biosensors based on oxidases. *Sens. Actuat. B* **2007**, *124*, 297-302.
72. Schwarz, J.; Kaden, H.; Kutschke, S.; Glombitza, F. Potentiometrische Biosensoren zur Bestimmung von Metallkationen. *GIT Labor-Fachzeitschrift* **2007**, *51*, 408-409.
73. Perley, G.A.; Godshalk, J.B. Cell for pH measurements. *US 2 416 949*, 1947.
74. Widera, J.; Riehl, B.L.; Johnson, J.M.; Hansen, D.C. State-of-the-art monitoring of fuel acidity. *Sens. Actuat. B* **2008**, *130*, 871-881.
75. Kress-Rogers, E. Solid-state pH sensors for food applications. *Trends Food Sci. Technol.* **1991**, *12*, 320-324.
76. de Rooij, N.F.; Bergvelt, P. *Monitoring Vital Parameters during Extracorporeal Circulation*, Kimmich, H.P., Ed.; Kaerge: Basel, Switzerland, 1981.
77. Glab, S.; Hulanicki, A.; Edwall, G.; Ingman, F. Metal-metal oxide and metal oxide electrodes as pH sensors. *Crit. Rev. Anal. Chem.* **1989**, *21*, 29-47.
78. Kinlen, P.J.; Heider, J.E.; Hubbard, D.E. A solid-state pH sensor based on a Nafion-coated iridium oxide indicator electrode and a polymer-based silver chloride reference electrode. *Sens. Actuat. B* **1994**, *22*, 13-25.
79. Radiometer (electrode maker). *Růžička electrode*. Radiometer: Copenhagen, Denmark, 1990.
80. Oelßner, W.; Kaden, H. Iridiumdioxid-pH-Elektroden in Dickfilmtechnik. In *Elektrochemie der Ionenleiter*, Beck, E., Ed.; GDCh-Monographie: Frankfurt/Main, Germany, 1995; Vol. 3, pp. 390-392.
81. Kessel, R.; Drägerwerk, A.G. Amperometric sensor. *US Pat. 5518602*, 1996.
82. West, W.; Buehler, M.; Keymeulen D. *Metal/Metal Oxide Differential Electrode pH Sensors*. NASA's Jet Propulsion Laboratory: Pasadena, CA, 2007. Available online: [www.techbriefs.com/component/content/article/2287](http://www.techbriefs.com/component/content/article/2287) (accessed on 19 May 2009).
83. Kinoshita, E.; Ingman, F.; Edwal, G.; Thulin, S.; Glab, S. Polycrystalline and monocrystalline antimony, iridium and palladium as electrode material for pH-sensing electrodes. *Talanta* **1986**, *33*, 125-134.
84. Katsube, T.; Lauks, I.; Zemel, J.N. pH-Sensitive sputtered iridium oxide films. *Sens. Actuat. B* **1982**, *2*, 399-410.

85. El-Giar, E.E.M.; Wipf, D.O. Microparticle-based iridium oxide ultramicroelectrodes for pH sensing and imaging. *J. Electroanal. Chem.* **2007**, *609*, 147-154.
86. Pan, C.W.; Chou, J.C.; Sun, T.P.; Hsiung, S.K. Development of the tin oxide pH electrode by the sputtering method. *Sens. Actuat. B* **2005**, *108*, 863-869.
87. Tsai, C.N.; Chou, J.C.; Sun, T.P.; Hsiung, S.K. Study on the sensing characteristics and hysteresis effect of the tin oxide pH electrode. *Sens. Actuat. B* **2005**, *108*, 877-882.
88. Yin, L.T.; Chou, J.C.; Chung, W.Y.; Sun, T.P.; Hsiung, S.K. Study on separate structure extended gate H<sup>+</sup>-ion sensitive field effect transistor on a glass substrate. *Sens. Actuat. B* **2000**, *71*, 106-111.
89. Eftekhari, A. pH Sensor based on deposited film of lead dioxide on aluminium substrate electrode. *Sens. Actuat. B* **2003**, *88*, 234-238.
90. Kinoshita, K.; Madou, M.J. Electrochemical measurement on Pt, Ir and Ti oxides as pH probes. *J. Electrochem. Soc.* **1984**, *131*, 1089-1094.
91. Pocrifka, L.A.; Goncalves, C.; Grossi, P.; Colpa, P.C.; Pereira, E.C. Development of RuO<sub>2</sub>-TiO<sub>2</sub> (70-30) mol% for pH measurements. *Sens. Actuat. B* **2006**, *113*, 1012-1016.
92. Qingwen, L.; Yiming, W.; Guoan, L. pH-response of nanosized MnO<sub>2</sub> prepared with solid state reaction route at room temperature. *Sens. Actuat. B* **1999**, *59*, 42-47.
93. Kinoshita, E.; Ingman, F.; Edwall, G.; Glab, S. An examination of the palladium/palladium oxide system and its utility for pH-sensing electrodes. *Electrochim. Acta* **1986**, *31*, 29-35.
94. Niedrach, L.W. Oxygen ion-conducting ceramics: A new application in High-Temperature-High-Pressure pH sensors. *Science* **1980**, *207*, 1200-1202.
95. Seyfried, W.E.; Zhang, Z.; Ding, K. metal/metal oxide electrode as pH-sensor and methods of production. *Patent WO 02095386*, 2002.
96. Gao Pengtao, M.L.J.; Dos Santos, M.P.; Teixeira, V.; Andritschky, M. Characterization of ZrO<sub>2</sub> films prepared by rf reactive sputtering at different O<sub>2</sub> concentrations in the sputtering gases. *Vacuum* **2000**, *56*, 143-148.
97. Chiang, J.L.; Chen, Y.C.; Choul, J.C.; Cheng, C.C. Temperature effect on AlN/SiO<sub>2</sub> gate pH-ion-sensitive field-effect transistor devices study on the pH-sensing characteristics of ISFET with aluminium nitride membrane. *Jpn. J. Appl. Phys.* **2002**, *41*, 541-545.
98. Starr, S. *Novel materials for pH sensors*. Master thesis. University of Applied Sciences: Amberg, Germany, 2009.
99. Winsel, A. Hydrogen rod electrode with integrated hydrogen source. *US Pat. 5,407,555*, 1995.
100. Ives, D.J.G.; Janz, G.J. *Reference Electrodes*; Academic Press: New York, NY, USA, 1961.
101. Huang, I.Y.; Huang, R.S.; Lo, L.H. Improvement of integrated Ag/AgCl thin-film electrodes by KCl-gel coating for ISFET applications. *Sens. Actuat. B* **2003**, *94*, 53-64.
102. Cranny, A.; Atkinson, J.K. Thick film silver-silver chloride reference electrodes. *Meas. Sci. Technol.* **1998**, *9*, 1557-65.
103. Arevalo, A.; Souto, R.M.; Arevalo, M.C. Preparation and reproducibility of a silver-silver chloride electrode. *J. Applied Electrochem.* **1985**, *15*, 727-735.

104. Nikolskii, B.P.; Materova, E.A. Solid contact in membrane ion-selective electrodes. *Ion Sel. Electrode Rev.* **1985**, *7*, 3-39.
105. Vonau, W.; Oelßner, W.; Guth, U.; Henze, J. An all-solid-state reference electrode. *Sens. Actuat. B* **2009**, doi:10.1016/j.snb.2008.12.001.
106. Shuk, P.; Guth, U.; Greenblatt, M. Ion selective sensors based on molybdenum bronzes. *Solid State Electrochem.* **2002**, *8*, 374-383.
107. Gabel, J.; Vonau, W.; Shuk, P.; Guth, U. New reference electrodes based on tungsten-substituted molybdenum bronzes. *Solid State Ionics* **2004**, *169*, 75-80.
108. Guitton, J.; Forestier, M.; Kahil, H. New positive electrode for a rechargeable electrochemical generator and process for its manufacture. *French patent, FR 2547678*, 1984.
109. Noll, A.; Rudolf, V.; Grabner, E.W. A glass electrode with solid internal contact based on Prussian blue. *Electrochim. Acta* **1998**, *44*, 415-419.
110. Kurzweil, P.; Fischle, H.-J. A new monitoring method for electrochemical aggregates by impedance spectroscopy. *J. Power Sources* **2004**, *127*, 331-340.
111. Rezvani, B.; Lomibao, J.; Feng C.D. Impedance measurement of a pH electrode. *WO 2008021546*, 2008.

© 2009 by the authors; licensee Molecular Diversity Preservation International, Basel, Switzerland. This article is an open-access article distributed under the terms and conditions of the Creative Commons Attribution license (<http://creativecommons.org/licenses/by/3.0/>).